*Biochimica et Biophysica Acta*, 339 (1974) 164–172


BBA 76590

# THEORETICAL ANALYSIS OF THE MOLECULAR MOTION OF SPIN LABELS IN MEMBRANES

## ESR SPECTRA OF LABELED *BACILLUS SUBTILIS* MEMBRANES

JACOB ISRAELACHVILI, JAN SJÖSTEN, L. E. GÖRAN ERIKSSON, MAGDALENA EHRSTRÖM, ASTRID GRÄSLUND and ANDERS EHRENBERG*

*Department of Biophysics, Stockholm University, Arrhenius Laboratory, S-104 05 Stockholm (Sweden)*

(Received October 15th, 1973)

SUMMARY

Electron spin resonance (ESR) spectral line shapes are calculated for a nitroxide radical undergoing rapid motion within a cone. The analysis is correct to second order, and explicit expressions are derived for the hyperfine splittings and $g$-values by averaging both the secular and pseudosecular terms within the Hamiltonian. The simulated spectra are found to closely resemble those observed experimentally over a wide range of temperatures for stearic acid spin labels in cytoplasmic membranes of *Bacillus subtilis*. The present approach offers a simple, yet realistic way of interpreting spectra of nitroxide spin labels such as fatty acids and steroids when the motion is anisotropic.

## INTRODUCTION

There is today a wealth of experimental information on various nitroxide spin labels incorporated into biological structures such as membranes and model bilayers [1]. However, analysis and interpretation of the ESR spectra of nitroxide labels is often hampered by a lack of simple mathematical models which realistically describe the motion of spin labels and which are at the same time amenable to easy computation. The present analysis is based on a model where the spin labels are rotating rapidly and randomly within the confines of a cone of variable semi-cone angles. This model is not new [2–4, 8], though previous analyses have been approximate in that the averaging over angles has been performed on the final expresssions for the first order energy. Here we find that on averaging within the Hamiltonian one obtains explicit expressions for the hyperfine splittings and $g$-values that are correct to second order, and that allow for easy spectral simulations.

Simulated spectra based on the present model are concordant with published experimental spectra taken at different temperatures as well as with our own spectra on membranes of *Bacillus subtilis*, labeled with the stearic acid spin labels $I(m,n)$.

* All correspondence to Professor A. Ehrenberg.

I(m,n)

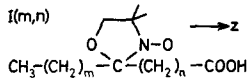


## THEORETICAL BASIS

The spin-Hamiltonian of a nitroxide radical in the laboratory XYZ coordinate system is adequately described by

$$\mathscr{H} = \beta_e \boldsymbol{H} \cdot g \cdot S + S \cdot T \cdot I \tag{1}$$

where $\beta_e$ is the Bohr magneton, $\boldsymbol{H}$ the external magnetic field, $g$ the electron $g$-value tensor, $S$ the electron spin operator, $T$ the hyperfine tensor, and $I$ the nuclear spin operator. The $g$ and $T$ tensors in the laboratory XYZ coordinate system (defined by $\boldsymbol{H} = \boldsymbol{H}_Z$) are related to the principal molecular axes xyz (defined by the principal axis of the diagonal tensors $g$(xyz) and $T$(xyz) which are assumed to coincide) by [5, 6]

$$g = L \cdot g(\text{xyz}) \cdot L^{-1} \qquad T = L \cdot T(\text{xyz}) \cdot L^{-1} \tag{2}$$

where $L$ is the rotational transformation matrix in terms of the three Eulerian angles $\theta$, $\phi$, $\psi$ (Fig. 1):

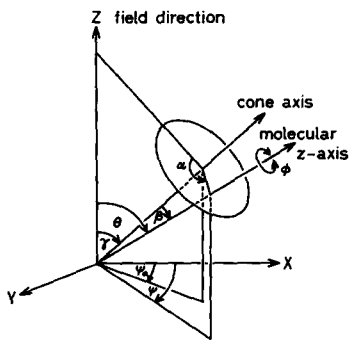


Fig. 1. Rapid motion within a cone model: $\gamma$ is the angle between the fixed cone axis and the external field direction Z; $\beta$ is the instantaneous angle between the molecular z-axis and the cone axis; $\theta$ is the instantaneous angle between the molecular z-axis and the external field direction Z; $\alpha$ is the instantaneous angle between the plane containing the z-axis and the cone axis and that containing the Z-axis and the cone axis; $\psi_0$ is the fixed angle between the projection of the fixed cone axis on the XY plane and the X-axis, and $\psi$ is the instantaneous angle between the projection of the z-axis and the X-axis on the XY plane. $\theta$ is related to $\gamma$, $\beta$ and $\alpha$ by Eqn (11), and $\psi$ is related to $\psi_0$, $\beta$, $\alpha$ and $\theta$ by Eqn (14). The averaging over $\theta$ and $\psi$, is effected by allowing $\alpha$ and $\beta$ to take on all values between 0 and $2\pi$, and 0 and $\beta_0$, respectively. (Note the left-handed axes system.)

$$L = \begin{pmatrix} \cos\theta\cos\phi\cos\psi - \sin\phi\sin\psi & \cos\theta\cos\psi\sin\phi + \sin\psi\cos\phi & \cos\psi\sin\theta \\ -\cos\theta\cos\phi\sin\psi - \sin\phi\cos\psi & -\cos\theta\sin\psi\sin\phi + \cos\phi\cos\psi & -\sin\theta\sin\psi \\ -\sin\theta\cos\phi & -\sin\theta\sin\phi & \cos\theta \end{pmatrix}$$

$\theta$ and $\psi$ are the spherical polar coordinates of the molecular z-axis relative to the external field direction (Z-axis), while $\phi$ represents rotations of the molecule about its own z-axis at constant $\theta$ and $\psi$.

For the electron spin quantized along the external field direction Z, Eqn (1) may be written as

$$\mathscr{H} = \beta_e \boldsymbol{H}_Z g_{ZZ} S_Z + S_Z(T_{XZ} I_X + T_{YZ} I_Y + T_{ZZ} I_Z) \tag{3}$$

where from Eqn (2)

$$\begin{aligned}
T_{XZ} &= (T_{xx} - T_{yy})\sin\theta\sin\phi(\cos\theta\sin\phi\cos\psi + \cos\phi\sin\psi) + (T_{zz} - T_{xx})\cos\theta\sin\theta\cos\psi \\
T_{YZ} &= (T_{xx} - T_{yy})\sin\theta\sin\phi(\cos\phi\cos\psi - \sin\phi\cos\theta\sin\psi) - (T_{zz} - T_{xx})\cos\theta\sin\theta\sin\psi \\
T_{ZZ} &= T_{xx}\sin^2\theta\cos^2\phi + T_{yy}\sin^2\theta\sin^2\phi + T_{zz}\cos^2\theta \\
g_{ZZ} &= g_{xx}\sin^2\theta\cos^2\phi + g_{yy}\sin^2\theta\sin^2\phi + g_{zz}\cos^2\theta
\end{aligned} \tag{4}$$

For nuclear spin $I = 1$, the eigenstates of the Hamiltonian, Eqn (3), have eigenenergies, $E_0$, $E_{+1}$, $E_{-1}$, given by

$$\begin{aligned}
E_0 &= \beta_e \boldsymbol{H}_Z g_{ZZ} = \beta_e \boldsymbol{H}_Z(g_{xx}\sin^2\theta\cos^2\phi + g_{yy}\sin^2\theta\sin^2\phi + g_{zz}\cos^2\theta) \\
E_{\pm 1} &= E_0 \pm (T_{XZ}{}^2 + T_{YZ}{}^2 + T_{ZZ}{}^2)^{1/2} \\
&= E_0 \pm (T_{xx}{}^2\sin^2\theta\cos^2\phi + T_{yy}{}^2\sin^2\theta\sin^2\phi + T_{zz}{}^2\cos^2\theta)^{1/2}
\end{aligned} \tag{5}$$

Eqn (5) is generally applicable to those radicals (including nitroxide radicals) where the local or hyperfine field at the nucleus, $\boldsymbol{H}_{hf}$, is much greater than the external field, i.e. $\boldsymbol{H}_{hf} \gg \boldsymbol{H}_Z$ [16]. In the case of a very strong external field ($\boldsymbol{H}_Z \gg \boldsymbol{H}_{hf}$), I is also quantized along Z and Eqn (5) becomes

$$E_0 = \beta_e \boldsymbol{H}_Z g_{ZZ} \quad E_{\pm 1} = E_0 \pm T_{ZZ} \tag{6}$$

If the molecule is not fixed but is undergoing rapid rotational motion restricted within certain angular limits each term of Eqn (4) must first be averaged over the allowed orientations, and Eqn (5) may then be written in the form

$$E_0 = \beta_e \boldsymbol{H}_Z \langle g_{ZZ} \rangle = \beta_e \boldsymbol{H}_Z g' \tag{7}$$

$$E_{\pm 1} = E_0 \pm (\langle T_{XZ} \rangle^2 + \langle T_{YZ} \rangle^2 + \langle T_{ZZ} \rangle^2)^{1/2} = E_0 \pm T' \tag{8}$$

where $\langle\ \rangle$ indicates partial or complete averaging over the allowed orientations $\theta$, $\phi$ and $\psi$, and where $g'$ and $T'$ may be thought of as the effective values of $g$ and $T$.

For a nitroxide spin label attached to a fatty acid chain, $I$(m,n), which rotates rapidly about the molecular z-axis, (see Fig. 1), we may average over all angles $\phi$ in Eqn (4). The effective $g$- and $T$-values may now be written as

$$g' = g_\perp + (g_{||} - g_\perp)\langle \cos^2\theta \rangle \tag{9}$$

$$\begin{aligned}
T' = [&\{T_\perp + (T_{||} - T_\perp)\langle \cos^2\theta \rangle\}^2 \\
&+ (T_{||} - T_\perp)^2\{\langle \cos\theta\sin\theta\sin\psi \rangle^2 + \langle \cos\theta\sin\theta\cos\psi \rangle^2\}]^{1/2}
\end{aligned} \tag{10}$$

where $T_{||} = T_{zz}$, $T_\perp = \frac{1}{2}(T_{xx} + T_{yy})$, $g_{||} = g_{zz}$ and $g_\perp = \frac{1}{2}(g_{xx} + g_{yy})$. In the strong field case $\boldsymbol{H}_Z \gg \boldsymbol{H}_{hf}$ while the expression for $g'$ is unchanged, that for $T'$ does not have the second (pseudosecular) term in curly brackets in Eqn (10).

*Rapid motion within a cone model*

We shall adopt a model [2–4] in which the molecular z-axis is tumbling rapidly within the confines of a cone of semi-cone angle $\beta_0$, and where the cone axis subtends

a fixed angle $\gamma$ to the external field $\boldsymbol{H}_Z$ (Fig. 1). After some straightforward trigonometrical manipulation we find

$$\cos\theta = \cos\gamma\cos\beta + \sin\gamma\sin\beta\cos\alpha \tag{11}$$

Thus:

$$\begin{aligned}<\cos^2\theta> &= \int_0^{2\pi} \mathrm{d}\alpha \int_0^{\beta_0} \cos^2\theta \cdot \sin\beta \cdot \mathrm{d}\beta \Big/ \int_0^{2\pi} \mathrm{d}\alpha \int_0^{\beta_0} \sin\beta \cdot \mathrm{d}\beta \\ &= \tfrac{1}{6}\{2-\cos\beta_0-\cos^2\beta_0+3\cos^2\gamma(1+\cos\beta_0)\cos\beta_0\}\end{aligned} \tag{12}$$

Eqn (12) may be substituted into Eqn (9) to yield an explicit expression for the effective $g$-value:

$$g'(\gamma,\beta_0) = g_\perp + \tfrac{1}{6}(g_{||}-g_\perp)\{2-\cos\beta_0-\cos^2\beta_0+3\cos^2\gamma(1+\cos\beta_0)\cos\beta_0\} \tag{13}$$

Eqn (13) reduces to expressions previously derived by Jost et al. [3] for $\gamma = 0$, $\gamma = 90\,^\circ$.

A further relation between the angles of Fig. 1

$$\sin(\psi-\psi_0) = \sin\beta\sin\alpha/\sin\theta \tag{14}$$

is required in order to evaluate the second term in curly brackets in Eqn (10), and after some algebra we find

$$<\cos\theta\sin\theta\sin\psi>^2 + <\cos\theta\sin\theta\cos\psi>^2 = \tfrac{1}{4}\{\cos\gamma\sin\gamma\cos\beta_0(1+\cos\beta_0)\}^2 \tag{15}$$

Eqns (15) and (12) may be substituted into Eqn (10) to yield an explicit expression for the effective $T$-value:

$$\begin{aligned}T'(\gamma,\beta_0) = [&\{T_\perp + \tfrac{1}{6}(T_{||}-T_\perp)(2-\cos\beta_0-\cos^2\beta_0+3\cos^2\gamma(1+\cos\beta_0)\cos\beta_0)\}^2 \\ &+\{\tfrac{1}{2}(T_{||}-T_\perp)\cos\gamma\sin\gamma\cos\beta_0(1+\cos\beta_0)\}^2]^{1/2}\end{aligned} \tag{16}$$

For no motion ($\beta_0 = 0$)

$$T'(\gamma,0) = [T_\perp{}^2\sin^2\gamma + T_{||}{}^2\cos^2\gamma]^{1/2}$$

For rapid isotropic motion ($\beta_0 = 180\,^\circ$)

$$T'(\gamma,180\,^\circ) = \tfrac{1}{3}(T_{||}+2T_\perp)$$

For any given $\beta_0$ the two orientations $\gamma = 0$ and $\gamma = 90\,^\circ$ correspond to those of maximum and minimum $T'$. These may be defined by $T_{||}'$ and $T_\perp'$ (see Fig.2) where from Eqn (16)

$$T_{||}' = T'(0,\beta_0) = T_\perp + \tfrac{1}{3}(T_{||}-T_\perp)(1+\cos\beta_0+\cos^2\beta_0) \tag{17}$$

$$T_\perp' = T'(90^\circ,\beta_0) = T_\perp + \tfrac{1}{6}(T_{||}-T_\perp)(2-\cos\beta_0-\cos^2\beta_0) \tag{18}$$

These values coincide with those previously obtained by Jost et al. [3] on the basis of an approximate analysis based, essentially, on Eqn (6) which is only valid for strong external field $\boldsymbol{H}_Z \gg \boldsymbol{H}_{hf}$. It is only at $\gamma = 0$ and $\gamma = 90\,^\circ$ (when the second term in curly brackets in Eqn (16) vanishes) that the strong and weak field values of $T'$ (i.e. $T_{||}'$ and $T_\perp'$) coincide; at any other value for $\gamma$ the weak field $T'$ will be greater than the strong field $T'$.

From Eqns (17) and (18) we obtain for the order parameter [3]

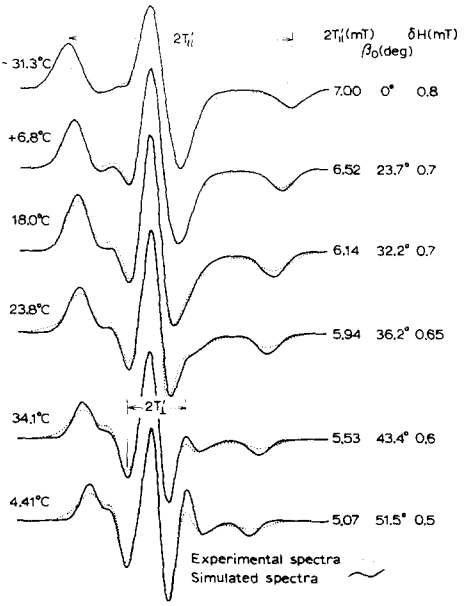


Fig. 2. Experimental first derivative spectra of the stearic acid spin label *I*(12,3) in cytoplasmic membranes of *B. subtilis* in 0.1 M NaCl solution, at different temperatures. For accurate measurements the outermost spectral singularities were recorded with high gain and slow sweep-time; this allowed determination of the spacings $2T_{\parallel}'$ to within $\pm 0.01$ mT. The measured values of $2T_{\parallel}'$ are somewhat larger than those normally observed, and imply that the nitroxide radical is in a very polar environment. (–) Simulated spectra based on the present "rapid motion within a cone model". $\delta H$ is the intrinsic Gaussian linewidth. Experimental and theoretical spectral pairs have been scaled to the same central peak-to-peak height.

$$S = \frac{T'_{\parallel} - T_{\perp}'}{T_{\parallel} - T_{\perp}} = (1/2)\cos\beta_0(1+\cos\beta_0) \tag{19}$$

From Eqn (17) the order parameter may also be expressed only in terms of $T_{\parallel}'$

$$S = \tfrac{1}{2}\left\{\frac{3(T_{\parallel}' - T_{\perp})}{(T_{\parallel} - T_{\perp})} - 1\right\} \tag{20}$$

which may be used on all spectra, and is particularly useful in cases where $T_{\perp}'$ is not measurable from experimental spectra as often happens. Eqn (20) is valid for all models, including the present, where

$$T_{\parallel}' + 2T_{\perp}' = T_{\parallel} + 2T_{\perp} = Tr\{T\} \tag{21}$$

It is sometimes useful to define the mobility of rotating spin label probes in terms of the simultaneous inward shifts of the high and low field extrema of the derivative spectrum [7]. From Eqns (7), (8), (13) and (17) we find that for the rapid motion within a cone model these shifts are given to within approx. 0.25% by

$$\text{high field shift: } \Delta H_{-1} = (1/3)\,(\Delta T - h\nu\Delta g/\beta_e g_{\parallel}^2)\,(2-\cos\beta_0-\cos^2\beta_0) \tag{22}$$

$$\text{low field shift: } \Delta H_{+1} = (1/3)\,(\Delta T + h\nu\Delta g/\beta_e g_{\parallel}^2)\,(2-\cos\beta_0-\cos^2\beta_0) \tag{23}$$

where $\nu$ is the microwave frequency, $\Delta g = g_{||} - g_{\perp}$, and $\Delta T = T_{||} - T_{\perp}$. In particular, the ratio of the high and low field shifts is found to be constant and is given by

$$\frac{\Delta H_{-1}}{\Delta H_{+1}} = \frac{1 - h\nu\Delta g/\beta_e \Delta T g_{||}^2}{1 + h\nu\Delta g/\beta_e \Delta T g_{||}^2} \tag{24}$$

for all $\beta_0$. For example, using typical values: $\nu = 9 \cdot 10^9$ Hz, $\Delta g = -0.0052$, $\Delta T = 2.5$ mT, $g_{||} = 2.0021$, we find $(\Delta H_{-1}/\Delta H_{+1}) = 2.0$. This value is very close to values predicted by the slow rotational diffusion analysis in the very slow motion region ($\tau_c > 2 \cdot 10^{-8}$ s) [7]. Thus it may not always be possible to distinguish between these two types of motion by simply measuring the simultaneous shifts of the high and low field extrema.

The present model is readily applicable to steroid spin labels (e.g. cholestane). Here the nitroxide radical is firmly attached to the steroid molecule in such a way that the hyperfine splitting along the molecular z-axis (the steroid long axis) is $T_{yy}$, whereas the splittings perpendicular to the molecular z-axis are $T_{xx}$ and $T_{zz}$. It should be noted that the z-axis is again chosen as the molecular axis over which the averaging within the cone is performed (see Fig. 1).

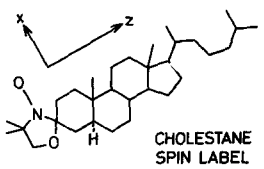

CHOLESTANE SPIN LABEL

For steroid spin labels, therefore, Eqn (4) must be rewritten with $T_{zz}$ and $T_{yy}$, and $g_{zz}$ and $g_{yy}$, interchanged. On the assumption that the steroid molecule is rotating rapidly about its molecular z-axis, we may average over all angles $\phi$ in Eqn (4), and the effective $g$- and $T$-values are still given by Eqns (13) and (16) but now $T_{||} = T_{yy}$, $T_{\perp} = \frac{1}{2}(T_{zz} + T_{xx})$, $g_{||} = g_{yy}$ and $g_{\perp} = \frac{1}{2}(g_{zz} + g_{xx})$.

Eqn (16) now yields values for $T'(0,\beta_0)$ and $T'(90\,°,\beta_0)$ that coincide with those derived by Lapper et al. [4], who extended the analysis of Jost et al. [3] to the cholestane spin label*.

## EXPERIMENTAL PROCEDURE

*B. subtilis* strain 168 was grown in 3 litre batches of synthetic medium with vigorous shaking. The cells were harvested during the stationary phase (16–18 h) and membrane ghosts prepared by lysozyme-DNAase treatment as described by Bishop et al. [9]. The spin labels *I*(12,3), *I*(5,10) and *I*(2,14) were purchased from SYVA, Palo Alto, Calif. The membranes were labeled by exchange from bovine serum albumin in 145 mM NaCl solution for 10 min. The mixture was then centrifuged at 30 000

* If rapid motion about the molecular z-axis is restricted, so that the averaging over $\phi$ is incomplete, the analysis must now include axial anisotropy about the molecular z-axis and becomes more complicated. A complete analysis, including axial rotations, will be reported in due time. In the case of nitroxide spin labels attached to fatty acid chains, however, the resulting spectra are not expected to be significantly modified.

$\times g$ for 20 min and the pellet washed twice and finally resuspended in 0.1 M salt solution. The pH values of the suspensions were close to 6. The final amount of spin labels in the membranes were less than 1% of the total lipid weight. ESR measurements were carried out with a Varian E-9 X-band spectrometer using a rectangular cavity and quartz sample tubes with 1 mm inner bore. The temperature was regulated with a heater-sensor system using cold nitrogen gas, and the sample temperature was measured with a platinum resistance to $\pm 0.3$ °C. Simulated ESR spectra were computed on an IBM 360.

## RESULTS AND DISCUSSION

Cytoplasmic membrane ghosts of *B. subtilis* 168 prepared as described above have been reported [9] to contain protein (62%), RNA (22%) and lipids (16%). 75% of the lipids are phospholipids, mainly diphosphatidylglycerol (49%) and phosphatidylethanolamine (34%), with 15 or 17 carbon atoms in their hydrocarbon chains. No unsaturated fatty acids are present, though 75% of the phospholipids have a methyl branch in their chains.

### *Experimental spectra*

Labeled membranes and protoplasts exhibited very similar spectra. However, the spin labels in protoplasts (and in intact bacteria) are reduced, and the ESR signals disappear within about 1 h at room temperature. Experiments were therefore carried out on labeled membranes only.

Although the lipid content of the membranes is very low (about 16%), there is strong experimental evidence that the stearic acid spin labels reside in lipid bilayer regions in the membranes. For example, we have observed some spectral anisotropy with the membranes oriented on a flat glass surface, similar to that previously observed with oriented lipid bilayers [1]. In addition, the increased mobilities of the spin labels in the order $I(12,3)$, $I(5,10)$ and $I(2,14)$ in the membranes is also consistent with a lipid bilayer structure.

Fig. 2 (dotted lines) shows a number of selected experimental spectra obtained with membranes containing $I(12,3)$ in 0.1 M NaCl solution at different temperatures. The top spectrum corresponds to a powder spectrum where the spin labels are almost completely immobilized. There is a gradual increase in the mobility of the labels as the temperature is raised, reflected by a gradual decrease in the value of $2T_{\parallel}'$. The spectra were completely reversible and no phase transitions were evident in the temperature range studied.

The order parameter S was evaluated from those spectra where $2T_{\perp}'$ was measurable, using Eqns (19) and (20), and it was found that these two equations yielded values for S that never differed by more than 0.03.

We have recently reported the effect of various anions and cations on such labeled membranes [10]. For membranes in 0.1 M $CaCl_2$ solution, for example, $2T_{\parallel}'$ is about 0.2 mT higher than in 0.1 M NaCl solution at 23 °C. But the variation of $2T_{\parallel}'$ with temperature in the two suspensions is practically the same, and indicates that the rigidity of the membranes in 0.1 M NaCl at a given temperature is the same as in 0.1 M $CaCl_2$ at a temperature that is 7 °C higher.

*Simulated spectra*

Fig. 2 (continuous lines) shows computer-simulated spectra based on the present model, each calculated at the value of $\beta_0$ that corresponds to the value of $T_{||}'$ of the experimental spectra using Eqn (17). Each spectrum was obtained by adding spectra at 2.5 ° intervals of $\gamma$, from $\gamma = 1.25$ ° to $\gamma = 88.75$ °, each weighted with $\sin \gamma$ (to account for the random distribution of cone axes in all directions). The functions $g'(\gamma,\beta_0)$ and $T'(\gamma,\beta_0)$ were calculated at the appropriate values of $\gamma$ and $\beta_0$ from Eqns (13) and (16) using $g_\perp = 2.0073$, $g_{||} = 2.0021$, $T_\perp = 0.55$ mT, and $T_{||} = 3.50$ mT. An intrinsic Gaussian linewidth $\delta H$ was found to be slightly superior to a Lorentzian. The value of $T_{||} = 3.50$ mT was obtained from the top (powder) experimental spectrum of Fig. 2, for which $T_{||}' = T_{||}$. The values of $T_\perp$, $g_\perp$, $g_{||}$, and $\delta H$ were then obtained by a best fit spectral simulation. As a check, the top (powder) simulated spectrum was also obtained using the standard programme of Lefebvre and Maruani [11]. The optimal intrinsic linewidth $\delta H$ was found to fall progressively with increasing temperature (or $\beta_0$) as shown in Fig. 2.

Fig. 2 demonstrates that the present "rapid motion within a cone model" is able to account for the main spectral features over a wide temperature range. This is especially true for the splittings $T_{||}'$ and $T_\perp'$, for which the discrepancy between the experimental and simulated values was never greater than 0.015 mT. However, both the experimental and simulated values of $T_\perp'$ (as measured from the spectra) were found to be between 0 and 0.09 mT smaller than the theoretically expected values as calculated from Eqn (21). A similar discrepancy between the theoretical and simulated values of $T_\perp'$ has previously been noted by Hubbell and McConnell [12].

The most unsatisfactory feature of the simulated spectra appears at the low and high field extrema which become too pronounced as $\beta_0$ increases. This, too, is noticeable in previous simulations [12]. To overcome this complication an angle-dependent linewidth function may be introduced into the simulation programme [13]. Work is currently in progress to include time-dependent effects in the model, and preliminary results indicate that both the high and low field extrema are broadened as the cone angle $\beta_0$ increases; the effect being most pronounced at high field. Recently, an interesting set of spectra at various temperatures with I(12,3) in microsomal membranes has been reported [14], where the low and high field extrema are fairly pronounced and the spectra are more like those of Fig. 2.

The rapid motion within a cone model offers a simple yet physically realistic approach to the interpretation of ESR spectra of nitroxide spin labels in membranes and vesicles when the motion is fairly restricted. The model assumes (1) that the restricted motion of the probe within the membrane or vesicle is rapid, and (2) that the rotational motion of the vesicle is slow. From theoretical considerations of rotational diffusion [7] we find that if the vesicles are rotating with a rotational correlation time $\tau_c$ less than about $5 \cdot 10^{-6}$ s there will be an appreciable decrease in the value of $T_{||}'$ due to rotational diffusion effects. For vesicles in water their radius must therefore be greater than about 150 Å for rotational diffusion effects to be negligible [15].

The present model is mathematically sound for all values of $\beta_0$, from $\beta_0 = 0$ (no motion) to $\beta_0 = 180$ ° (rapid isotropic tumbling), though it may not always be physically realistic for very large values of $\beta_0$. Whether the nitroxide probe is an allowed perturbation on the system studied will not, unfortunately, become evident from the model alone. The present analysis may be readily extended to partially

oriented systems where the fixed cone axes have a weighted distribution about some direction within the system, e.g. a Gaussian distribution of orientations about the perpendicular to the surfaces of oriented bilayers.

ACKNOWLEDGEMENTS

We thank the European Molecular Biology Organization, the Swedish Natural Science Research Council, and the Swedish Medical Research Council for financial support, and Prof. H. M. McConnell, Stanford, for pointing out an error in an earlier manuscript.

REFERENCES

1 Schreier-Muccillo, S. and Smith, I. C. P. (1973) in Progress in Surface and Membrane Science (Danielli, J. F., Rosenberg, M. D. and Cadenhead, D. A., eds), Vol. 9, Academic Press, New York
2 Libertini, L. J., Waggoner, A. S., Jost, P. C. and Griffith, O. H. (1969) Proc. Natl. Acad. Sci. U.S. 64, 13–19
3 Jost, P., Libertini, L. J., Herbert, V. C. and Griffith, O. H. (1971) J. Mol. Biol. 59, 77–98
4 Lapper, R. D., Paterson, S. J. and Smith, I. C. P. (1973) Can. J. Biochem. 50, 969–981
5 Pedersen, J. B. (1972) J. Chem. Phys. 57, 2680–2683
6 Blinder, S. M. (1960) J. Chem. Phys. 33, 748–752
7 McCalley, R. C., Shimshick, E. J. and McConnell, H. M. (1972) Chem. Phys. Lett. 13, 115–119
8 Birrell, G. B., Van, S. P. and Griffith, O. H. (1973) J. Am. Chem. Soc. 95, 2451–2458
9 Bishop, D. G., Rutberg, L. and Samuelsson, B. (1967) Eur. J. Biochem. 2, 448–453
10 Ehrström, M., Eriksson, L. E. G., Israelachvili, J. and Ehrenberg, A. (1973) Biochem. Biophys. Res. Commun. 55, 396–402
11 Lefebvre, R. and Maruani, J. (1965) J. Chem. Phys. 42, 1480–1502
12 Hubbell, W. L. and McConnell, H. M. (1971) J. Am. Chem. Soc. 93, 314–326
13 Jost, P., Griffith, O. H., Capaldi, R. A. and Vanderkooi, G. (1973) Biochim. Biophys. Acta 311, 141–152
14 Stier, A. and Sackman, E. (1973) Biochim. Biophys. Acta 311, 400–408
15 Carrington, A. and McLachlan, A. D. (1969) Introduction to Magnetic Resonance, p. 189, Harper and Row, New York
16 Wertz, J. E. and Bolton, J. R. (1972) Electron Spin Resonance, Section 7-6, McGraw-Hill, New York